Accepted Manuscript

Discovery of *O* ^{6}-benzyl glaziovianin A, a potent cytotoxic substance and a potent inhibitor of α,β-tubulin polymerization

Ichiro Hayakawa, Shuya Shioda, Takumi Chinen, Taisei Hatanaka, Haruna Ebisu, Akira Sakakura, Takeo Usui, Hideo Kigoshi

PII: S0968-0896(16)30711-8
DOI: http://dx.doi.org/10.1016/j.bmc.2016.09.026
Reference: BMC 13279

To appear in: *Bioorganic & Medicinal Chemistry*

Received Date: 3 August 2016
Revised Date: 9 September 2016
Accepted Date: 10 September 2016

Please cite this article as: Hayakawa, I., Shioda, S., Chinen, T., Hatanaka, T., Ebisu, H., Sakakura, A., Usui, T., Kigoshi, H., Discovery of *O* ^{6}-benzyl glaziovianin A, a potent cytotoxic substance and a potent inhibitor of α,β-tubulin polymerization, *Bioorganic & Medicinal Chemistry* (2016), doi: http://dx.doi.org/10.1016/j.bmc.2016.09.026

Graphical Abstract

To create your abstract, type over the instructions in the template box below.
Fonts or abstract dimensions should not be changed or altered.

Discovery of O^6-benzyl glaziovianin A, a potent cytotoxic substance and a potent inhibitor of α,β-tubulin polymerization

Leave this area blank for abstract info.

Ichiro Hayakawa,* Shuya Shioda, Takumi Chinen, Taisei Hatanaka, Haruna Ebisu, Akira Sakakura, Takeo Usui,* Hideo Kigoshi*

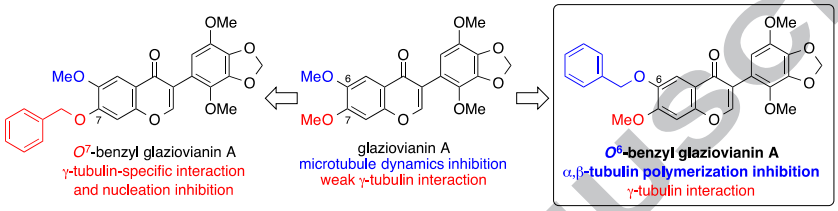

Bioorganic & Medicinal Chemistry
journal homepage: www.elsevier.com

Discovery of O^6-benzyl glaziovianin A, a potent cytotoxic substance and a potent inhibitor of α,β-tubulin polymerization

Ichiro Hayakawa[a]*, Shuya Shioda[b], Takumi Chinen[c], Taisei Hatanaka[a], Haruna Ebisu[c], Akira Sakakura[a], Takeo Usui[c]*, Hideo Kigoshi[b]*

[a]*Division of Applied Chemistry, Graduate School of Natural Science and Technology, Okayama University, 3-1-1 Tsushima-naka, Kita-ku, Okayama 700-8530, Japan*
[b]*Department of Chemistry, Graduate School of Pure and Applied Sciences, University of Tsukuba, 1-1-1 Tennodai, Tsukuba 305-8571, Japan*
[c]*Graduate School of Life and Environmental Sciences, University of Tsukuba, 1-1-1 Tennodai, Tsukuba 305-8572, Japan*

ARTICLE INFO

Article history:
Received
Received in revised form
Accepted
Available online

Keywords:
O^6-Benzyl glaziovianin A
Cytotoxicity
α,β-Tubulin inhibitor
Structure–activity relationship study

ABSTRACT

We have discovered O^6-benzyl glaziovianin A, which showed stronger inhibition of microtubule polymerization (IC_{50} = 2.1 μM) than known α,β-tubulin inhibitors, such as colchicine and glaziovianin A. Also, we performed competition binding experiments of O^6-benzyl glaziovianin A and revealed that O^6-benzyl glaziovianin A binds to the colchicine binding site with high affinity. It is interesting that glaziovianin A derivatives change their mode of action in benzylation at the O^6 (α,β-tubulin inhibitor) or O^7 (γ-tubulin-specific inhibitor) position.

1. Introduction

Inhibitors of microtubule polymerization are some of the most common and effective treatment for breast cancer.[1] Colchicine, vinca alkaloids, and taxol are known as typical microtubule inhibitors of natural product origin. Many kinds of inhibitors of microtubules bind to either the colchicine binding site,[2] the vinblastine binding site,[3] or the taxoid binding site[4] in α,β-tubulin. Especially, taxanes and vinca alkaloids, such as taxol and vinblastine, are used in cancer chemotherapy. In contrast, inhibitors binding to the colchicine site has not been used in clinic at the present, although these compounds are currently undergoing clinical development and evaluation in patients with a wide array of cancers.

Glaziovianin A (**1**), a naturally occurred isoflavone derivative, is an inhibitor of microtubule dynamics (Fig. 1).[5,6] Previously, we reported the synthesis[7] and structure–activity relationship study[8] of glaziovianin A (**1**). In that report, we revealed that O^7-alkylated[9] glaziovianin A analogues have strong cytotoxicity against HeLa cells. Especially, O^7-propargyl glaziovianin A (**2**) indicated more potent cytotoxic effects[8b] than glaziovianin A (**1**) itself and decreased the polymerization rate of α,β-tubulin *in vitro*.[6] We also revealed, from the results of a competition assay, that glaziovianin A (**1**) binds to the colchicine site of α,β-tubulin.[6]

In a series of structure–activity relationship studies of glaziovianin A (**1**), we reported the synthesis of O^7-benzyl glaziovianin A (**3**), which showed strong cytotoxicity against HeLa cells (IC_{50} = 0.19 μM).[8] On the other hand, we recently developed a modified route to the synthesis of O^7-modified glaziovianin A.[7b] However, the resultant O^7-benzyl glaziovianin A (**3**) showed much weaker cytotoxicity (IC_{50} = 12.81 μM). We supposed that the previous lot of O^7-benzyl glaziovianin A (**3**) contained an impurity that exhibits strong cytotoxicity. In this paper, we described the discovery of a new glaziovianin A derivative: O^6-benzyl glaziovianin A (**4**), which showed more potent cytotoxicity against HeLa cells and inhibitory activity of polymerization of α,β-tubulin than known α,β-tubulin inhibitors, such as colchicine and glaziovianin A (**1**).

O^6-benzyl glaziovianin A (**4**) R^1 = Me, R^2 = Bn

Figure 1. Structures of glaziovianin A (**1**) and its derivatives.

2. Results and Discussion

2.1. Discovery of O^6-benzyl glaziovianin A (4)

We used HPLC analysis to examine the purities of old and new lots of O^7-benzyl glaziovianin A (**3**) (Fig. 2). As a result, the previously synthesized O^7-benzyl glaziovianin A (**3**) contained an impurity (ca. 10%). In contrast, the new lot of O^7-benzyl glaziovianin A (**3**) did not contain this impurity.

Figure 2. HPLC analysis of O^7-benzyl glaziovianin A (**3**); upper: preparation by the previous synthetic route; bottom: preparation by the modified synthetic route (column: Develosil ODS-HG-5 (ϕ4.6 × 250 mm), solvent: 75% MeOH aq., detect: UV 254 nm, flow rate: 1 mL/min).

Next, we isolated the impurity in previously synthesized O^7-benzyl glaziovianin A (**3**) by using preparative HPLC and determined its structure. The molecular weight of the impurity was identical to that of O^7-benzyl glaziovianin A (**3**) by ESIMS analysis. Also, we compared the ^{1}H NMR data between the impurity and O^7-benzyl glaziovianin A (**3**) (Table 1). The chemical shifts of the protons at the A-ring portion (H_1–H_4) in the impurity were different from those of O^7-benzyl glaziovianin A (**3**), and the others corresponded well (within 0.01 ppm). These results suggested that the impurity was an isomer of O^7-benzyl glaziovianin A (**3**) concerning the A-ring, such as O^6-benzyl glaziovianin A (**4**). Thus, we planned to rigorously synthesize O^6-benzyl glaziovianin A (**4**) to confirm the structure of the impurity.

Table 1 ^{1}H NMR data of A-ring of O^7-benzyl glaziovianin A (**3**) and the impurity (600 MHz, CD_3OD)

	^{1}H (ppm)	
No.	O^7-benzyl glaziovianin A (**3**)	impurity
H_1	7.58	7.64
H_2	7.22	7.18
H_3	5.27	5.21
H_4	3.95	4.01

O^7-benzyl glaziovianin A (**3**)

We synthesized O^6-benzyl glaziovianin A (**4**) according to our established strategy (Scheme 1). To convert commercially available sesamol (**5**) to known benzophenone **6**, we followed the procedure reported by Tamura et al.[10] Regioselective methylation of benzophenone **6** gave the desired monomethyl benzophenone **7**,[11] which was converted into benzyl ether **8**. Condensation of **8** with *N*,*N*-dimethylformamide dimethyl acetal afforded enamine **9**, which was transformed into iodochromone **10**. The Suzuki–Miyaura coupling reaction[12] between iodochromone **10** and pinacol boronate **11**[7b] furnished O^6-benzyl glaziovianin A (**4**).

O^6-benzyl glaziovianin A (**4**)

Scheme 1. Synthesis of O^6-benzyl glaziovianin A (**4**). Reagents and conditions: (a) MeI, K_2CO_3, acetone, 60 °C; (b) BnCl, K_2CO_3, *n*-Bu_4NI, MeCN, rt, 35% in two steps; (c) $(MeO)_2CHNMe_2$, 95 °C; (d) I_2, py, $CHCl_3$, rt, 86% in two steps; (e) **11**, $PdCl_2(dppf)\cdot CH_2Cl_2$, 1 M Na_2CO_3 aq, 1,4-dioxane, rt, 76%.

The ^{1}H NMR data of the impurity were in good agreement with those of synthetic O^6-benzyl glaziovianin A (**4**) (Fig. 3). Therefore, the structure of the impurity was confirmed to be O^6-benzyl glaziovianin A (**4**).[13]

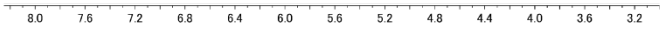

Figure. 3 ^{1}H NMR (600 MHz, CD_3OD) spectra of the impurity and of synthetic O^6-benzyl glaziovianin A (**4**).

2.2. Biological activity of O^6-benzyl glaziovianin A (4)

We next evaluated the cytotoxicity of O^6-benzyl glaziovianin A (**4**), O^7-benzyl glaziovianin A (**3**), and glaziovianin A (**1**) against HeLa cells (Table 2) and the effects on the microtubule polymerization (Fig. 4). Glaziovianin A (**1**) showed moderate, and O^7-benzyl glaziovianin A (**3**) weak cytotoxicity against HeLa cells. In contrast, O^6-benzyl glaziovianin A (**4**) showed potent cytotoxicity (IC_{50} = 0.07 μM).

Table 2 Cytotoxicity of colchicine and glaziovianin A derivatives against HeLa cells

compound	IC_{50} (μM)
colchicine	0.02 ± 0.01
glaziovianin A (**1**)	0.61 ± 0.07
O^7-benzyl glaziovianin A (**3**)	12.81 ± 6.26
O^6-benzyl glaziovianin A (**4**)	0.07 ± 0.01

Previously we reported that glaziovianin A (**1**) and O^7-propargyl glaziovianin A (**2**) decreased the *in vitro* polymerization rate of α,β-tubulin.[6] In the present study, we used microtubule polymerization to examine whether O^6-benzyl glaziovianin A (**4**) also inhibits microtubule dynamics. As shown in Fig. 4A, pure O^7-benzyl glaziovianin A (**3**) showed no apparent effects, but O^6-benzyl glaziovianin A (**4**) completely inhibited microtubule polymerization at the concentration of 3 μM. In the same condition, colchicine also inhibited microtubule polymerization, but less potently compared with O^6-benzyl glaziovianin A (**4**) (Fig. 4B). The IC_{50} values for O^6-benzyl glaziovianin A (**4**) and colchicine were 2.1 ± 0.7 and 9.1 ± 1.3 μM, respectively (Fig. 4B), suggesting that O^6-benzyl glaziovianin A (**4**) is a more potent microtubule inhibitor than colchicine *in vitro*. Furthermore, the previous lot of O^7-benzyl glaziovianin A (**3**) (before HPLC separation) still showed an intermediate inhibitory effect on microtubule polymerization (Fig. 4A). Therefore, we concluded that contaminating O^6-benzyl glaziovianin A (**4**) in the previous lot of O^7-benzyl glaziovianin A (**3**) caused considerable inhibitory activity against microtubule polymerization and cell proliferation.[14]

Figure 4. Effects of glaziovianin A derivatives on microtubule polymerization. Purified porcine tubulin was incubated with or without each compound at 37 °C and then polymerized by the addition of 10 μM taxol (**A**) or 1 M glutamate (**B**). **A.** O^6-Benzyl glaziovianin A (**4**) inhibited microtubule polymerization at 3 μM, but the O^7-derivative did not. ○: DMSO control; ●: O^7-benzyl glaziovianin A (**3**), which was prepared by the previous synthetic route (before HPLC separation); ■: HPLC-separated O^7-benzyl glaziovianin A (**3**); and □: HPLC-separated O^6-benzy glaziovianin A (**4**). **B.** O^6-Benzyl glaziovianin A (**4**) inhibited microtubule polymerization in a dose-dependent manner. Effects of O^6-benzyl glaziovianin A (**4**), prepared by the modified synthetic route, on microtubule polymerization *in vitro*. The final concentrations were 0 μM (○), 0.5 μM (▲), 1.5 μM (△), and 3.0 μM (◆) of O^6-benzyl glaziovianin A (**4**), 5 μM (■) and 30 μM (□) of colchicine, or 10 μM of glaziovianin A (**1**) (●).

2.3. Competition binding experiments of O^6-benzyl glaziovianin A (4)

We previously reported that glaziovianin A (**1**) and O^7-propargyl glaziovianin A (**2**) decreased the *in vitro* polymerization rate of α,β-tubulin by binding to the colchicine binding site.[6] To determine whether the binding site of O^6-benzyl glaziovianin A (**4**) is the same as that of glaziovianin A (**1**), we performed competition binding experiments using [^{3}H]-labeled vinblastine and colchicine (Table 3). Like colchicine and glaziovianin A (**1**), O^6-benzyl glaziovianin A (**4**) inhibited the binding of [^{3}H]-colchicine but enhanced the binding of [^{3}H]-vinblastine, suggesting that the binding site of O^6-benzyl glaziovianin A (**4**) is identical or close to those of colchicine and glaziovianin A (**1**). Furthermore, the changes in tryptophan fluorescence showed that O^6-benzyl glaziovianin A (**4**) bound to α,β-tubulin with a markedly higher affinity than glaziovianin A (**1**) and colchicine (Table 4). These results strongly suggest that O^6-benzyl glaziovianin A (**4**) binds to the colchicine binding site with high affinity and inhibits microtubule polymerization more potently than colchicine and glaziovianin A (**1**).

Table 3 Inhibitory effects of O^6-benzyl glaziovianin A (**4**) on the binding of colchicine and vinblastine to tubulin

	radiolabelled drug bound (% of control)	
compound	[^{3}H]-colchicine	[^{3}H]-vinblastine
colchicine	18.2 ± 1.1	151.9 ± 6.8
vinblastine	127. 1 ± 9.7	5.3 ± 0.5
glaziovianin A (**1**)	67.8 ± 7.1	112.4 ± 5.5
O^6-benzyl glaziovianin A (**4**)	20.3 ± 1.5	117.7 ± 4.4

The competition assay of O^6-benzyl glaziovianin A (**4**) binding to tubulin with radiolabelled vinblastine or colchicine was monitored by the centrifugal gel filtration method. Values are the means ± s.d.

Table 4 Drug binding analysis based on tryptophan fluorescence spectrum changes

compound	K_d (μM)
colchicine	26.6 ± 13.4
glaziovianin A (**1**)	80.0 ± 45.7
O^6-benzyl glaziovianin A (**4**)	1.0 ± 0.1

The K_d value of each drug was calculated from the tryptophan fluorescence decrease (ΔFL) from three independent experiments using GraphPad Prizm software. Values are the means ± s.d.

2.4. Effects of O^6-benzyl glaziovianin A (4) on the cell cycle progression and spindle structure in mitosis

We next examined the effects of O^6-benzyl glaziovianin A (**4**) on the cell cycle progression and spindle structure in mitosis (Fig. 5). O^6-Benzyl glaziovianin A (**4**) completely inhibited the cell cycle progression in mitosis at 10 times lower concentrations than glaziovianin A (**1**) did (Fig. 5, Left). Under this condition, O^6-benzyl glaziovianin A (**4**) inhibited the normal bipolar spindle formation (Fig. 5, Right). Most of the cells treated with 100 nM O^6-benzyl glaziovianin A (**4**) showed a multipolar spindle as the glaziovianin A (**1**)-treated cells did. At higher concentrations, O^6-benzyl glaziovianin A (**4**) completely disrupted the microtubule and only short fragments were observed. These results also indicate that O^6-benzyl glaziovianin A (**4**) is a potent microtubule polymerization inhibitor.

Figure 5. Effects of O^6-benzyl glaziovianin A (**4**) on cell cycle progression (Left) and spindle morphology (Right). Left: Effects of colchicine, glaziovianin A (**1**) and O^6-benzyl glaziovianin A (**4**) on cell cycle progression in HeLa cells. HeLa cells were treated with each compound for 18 h. Right: Effects of colchicine, glaziovianin A (**1**) and O^6-benzyl glaziovianin A (**4**) on spindle morphology in HeLa cells. HeLa cells were treated with glaziovianin A (**1**) and O^6-benzyl glaziovianin A (**4**) for 6 h. Scale bar, 20 μm. Green and blue represent α-tubulin and DNA, respectively.

3. Conclusions

In conclusion, we have discovered O^6-benzyl glaziovianin A (**4**), which showed stronger inhibition of microtubule polymerization than known α,β-tubulin inhibitors, such as colchicine and glaziovianin A (**1**).[15] O^6-Benzyl glaziovianin A (**4**) potently inhibited microtubule polymerization *in vitro* (IC_{50} = 2.1 μM) and arrested cell cycle progression in mitosis by forming abnormal spindles, suggesting that the introduction of a benzyl group at the O^6 position potentiates the affinity to the colchicine binding site of α,β-tubulin. Although O^6-benzyl glaziovianin A (**3**) inhibited microtubule polymerization *in vitro* more potently than colchicine, the cytotoxicity of O^6-benzyl glaziovianin A (**3**) was weaker than that of colchicine, suggesting that cell permeability of O^6-benzyl glaziovianin A (**3**) is lower than that of colchicine.

We recently reported glaziovianin A (**1**) and O^7-propargyl glaziovianin A (**2**) as microtubule dynamics inhibitors,[6] and O^7-benzyl glaziovianin A (**3**) as a γ-tubulin-specific inhibitor, gatastatin.[14] Our preliminary data suggested that O^6-benzyl glaziovianin A (**4**) also inhibits GTP binding on γ-tubulin (89.6 ± 1.7% inhibition at 60 μM). This inhibitory activity was weaker than that of O^7-benzyl glaziovianin A (**3**) (93.3 ± 3.7% inhibition at 60 μM). Thus, it is interesting that glaziovianin A derivatives change their mode of action in benzylation at the O^6 (α,β-tubulin and γ-tubulin inhibitor) or O^7 (γ-tubulin-specific inhibitor) position (Fig. 6).[14b] Here we showed that glaziovianin A (**1**) is good template with which to develop tubulin superfamily inhibitors. The synthesis of O^6-modified glaziovianin A derivatives is currently underway in our group.

Figure 6 Summary of the structure–activity relationships of glaziovianin A derivative.

4. Experimental

4.1. Chemistry

General method

All moisture-sensitive reactions were performed under an atmosphere of argon or nitrogen, and the starting materials were azeotropically dried with benzene or toluene before use. Anhydrous acetone, MeCN, $CHCl_3$, and 1,4-dioxane were purchased from Kanto Chemical Co., Inc., or Wako Pure Chemical Industries Ltd., and used without further drying. TLC analyses were conducted on E. Merck precoated silica gel 60 F_{254} (0.25 mm layer thickness). Merck silica gel 60 (0.040–0.063 mm 230–400 mesh) and Fuji Silysia silica gel BW-820MH (75–200 μm) were used for column chromatography. Melting points were measured on Yanaco MP-J3 micro melting point apparatus and are uncorrected. Infrared (IR) spectra were recorded on a JASCO FT/IR-4100 instrument and only selected peaks are reported in wavenumbers (cm^{-1}). ^1H and ^{13}C NMR spectra were recorded on a Varian INOVA-600 spectrometer, a Varian Mercury-400 spectrometer, a Bruker AVANCE 600 spectrometer, a Bruker AVANCE 400 spectrometer or a Bruker DPX 400 spectrometer. The ^1H and ^{13}C chemical shifts were referenced to the solvent peaks, δ_H 7.26 (residual $C\underline{H}Cl_3$) and δ_C 77.0 ppm ($\underline{C}DCl_3$), or δ_H 3.31 (residual $C\underline{H}D_2OD$) and δ_C 49.0 ppm ($\underline{C}D_3OD$), respectively. J values are given in Hz. The following abbreviations are used for spin multiplicity: s = singlet, d = doublet, t = triplet, q = quartet, m = multiplet, and br = broad.

High resolution ESI/TOF mass spectra were recorded on a JEOL AccuTOFCS JMS-T100CS spectrometer.

*4.1.1. 1-(5-(benzyloxy)-2-hydroxy-4-methoxyphenyl)ethan-1-one (**8**)*

To a stirred solution of benzophenone **6** (103 mg, 0.61 mmol) in acetone (3.0 mL) were added K_2CO_3 (172 mg, 1.25 mmol) and MeI (40 μL, 0.64 mmol) at room temperature. After being stirred at reflux for 4 h, the reaction mixture was concentrated. The resultant mixture was dissolved in H_2O (1.0 mL), diluted with 2 M HCl (0.3 mL) to pH 3, and extracted with EtOAc (3 × 12 mL). The combined extracts were washed with brine, dried (Na_2SO_4), filtered, and concentrated to give a crude monomethyl benzophenone **7** (110 mg), which was used for the next reaction without further purification.

To a stirred solution of the crude monomethyl benzophenone **7** (110 mg) in MeCN (3.0 mL) were added K_2CO_3 (165 mg, 1.19 mmol), BnCl (80 μL, 0.700 mmol), and *n*-Bu_4NI (329 mg, 0.89 mmol) at room temperature. After being stirred at room temperature for 8.5 h, the reaction mixture was filtrated with Celite, and this Celite was rinsed with EtOAc (4 × 10 mL). The filtrate and rinse were concentrated. The residual solid was purified by column chromatography on silica gel (10 g, hexane–EtOAc 16:1→14:1→12:1→2:1) to give acetophenone **8** (57.3 mg, 35% in two steps) as a white solid; mp 147–149 °C; IR ($CHCl_3$) 3025, 3012, 1633, 1508, 1444, 1374, 1329 cm^{-1}; ^1H NMR (400 MHz, $CDCl_3$) δ 12.59 (s, 1H), 7.45–7.32 (m, 5H), 7.09 (s, 1H), 6.46 (s, 1H), 5.08 (s, 2H), 3.92 (s, 3H), 2.44 (s, 3H); ^{13}C NMR (100 MHz, $CDCl_3$) δ 202.1, 160.4, 157.7, 140.4, 136.8, 128.6 (2C), 128.1, 127.6 (2C), 116.2, 111.7, 100.6, 72.6, 56.1, 26.2; HRMS (ESI) *m/z* 271.1001, calcd for $C_{16}H_{15}O_4$ $[M–H]^-$ 271.0975.

*4.1.2. 6-(benzyloxy)-3-iodo-7-methoxy-4H-chromen-4-one (**10**)*

Acetphenone **8** (6.5 mg, 24 μmol) was dissolved in *N*,*N*-dimethylformamide dimethyl acetal (0.10 mL, 0.75 mmol) and stirred at 95 °C for 2 h. The reaction mixture was concentrated *in vacuo* to give crude enamine **9** (10 mg), which was used for the next reaction without further purification.

To a stirred solution of crude enamine **9** (10 mg) in $CHCl_3$ (0.4 mL) were added pyridine (4.0 μL, 50 μmol) and I_2 (9.5 mg, 37 μmol) at 0 °C. After being stirred in dark at room temperature for 15 h, the mixture was diluted with saturated aqueous $Na_2S_2O_3$ (1 mL) at 0 °C and extracted with $CHCl_3$ (4 × 3 mL). The combined extracts were washed with brine, dried (Na_2SO_4), filtered, and concentrated. The residual solid was purified by column chromatography on silica gel (700 mg, $CHCl_3$) to give iodochromone **10** (8.4 mg, 86% in two steps) as a yellow solid: mp 129–132 °C; IR ($CHCl_3$) 3012, 1634, 1618, 1505, 1448, 1287, 1270 cm^{-1}; ^1H NMR (400 MHz, $CDCl_3$) δ 8.21 (s, 1H), 7.58 (s, 1H), 7.47 (d, *J* = 7.2 Hz, 2H), 7.39–7.28 (m, 3H), 6.86 (s, 1H), 5.21 (s, 2H), 3.96 (s, 3H); ^{13}C NMR (100 MHz, $CDCl_3$) δ 172.4, 156.9, 155.3, 152.4, 147.2, 136.0, 128.7 (2C), 128.2, 127.7 (2C), 115.1, 107.0, 99.6, 86.6, 71.2, 56.5.; HRMS (ESI) *m/z* 430.9744, calcd for $C_{17}H_{13}NaIO_4$ $[M+Na]^+$ 430.9750.

*4.1.3. O^6-benzyl glaziovianin A (**4**)*

All solvents were degassed by freeze–thawing. To a stirred solution of pinacol boronate **11** (8.4 mg, 24 μmol), iodochromone **10** (8.0 mg, 20 μmol), and $PdCl_2(dppf)\cdot CH_2Cl_2$ (3.5 mg, 4.3 μmol) in 1,4-dioxane (450 μL) was added aqueous 1 M Na_2CO_3 (150 μL, 150 μmol) at room temperature in a glove box. The mixture was stirred at room temperature under a stream of N_2 for 20 h and diluted with H_2O (1.0 mL) and $CHCl_3$ (3.0 mL) at room temperature. The layers were separated, and the aqueous layer was extracted with $CHCl_3$ (3 × 3.0 mL). The organic layer and extracts were combined, washed with brine, dried (Na_2SO_4), filtered, and concentrated. The residual solid was purified by column chromatography on silica gel (700 mg, hexane–EtOAc 4:1→1:1) to give O^6-benzyl glaziovianin A (**4**) (containing Pd-metal). The resultant mixture was dissolved in $CHCl_3$ (3 mL), and SiliaBond (SILICYCLE, SiliaMetS® Thiourea, 10 mg) was added. The resulting mixture was stirred at room temperature for 12 h, filtered, and concentrated. The resultant mixture was purified by recycle HPLC [JAIGEL-1H-40 (ϕ20 × 600 mm) and JAIGEL-2H-40 (ϕ20 × 600 mm); flow rate 3.8 mL/min; detection, UV 254 nm; solvent $CHCl_3$] to give O^6-benzyl glaziovianin A (**4**) (6.3 mg, 68%) as a white solid: mp 185–188 °C; IR ($CHCl_3$) 3026, 3003, 1636, 1606, 1506, 1451, 1296, 1270 cm^{-1}; ^1H NMR (400 MHz, $CDCl_3$) δ 7.89 (s, 1H), 7.71 (s, 1H), 7.48 (d, *J* = 7.2 Hz, 2H), 7.40–7.28 (m, 3H), 6.89 (s, 1H), 6.52 (s, 1H), 6.02 (s, 2H), 5.22 (s, 2H), 3.98 (s, 3H), 3.87 (s, 3H), 3.85 (s, 3H); ^{13}C NMR (100 MHz, $CDCl_3$) δ 175.4, 154.9, 153.5, 152.5, 146.8, 139.2, 139.0, 137.1, 136.8, 136.2, 128.7 (2C), 128.2, 127.7 (2C), 121.7, 118.1, 117.8, 110.2, 107.0, 101.9, 99.8, 71.1, 60.2, 56.9, 56.4; HRMS (ESI) *m/z* 485.1215, calcd for $C_{26}H_{22}NaO_8$ $[M+Na]^+$ 485.1206.

4.2. Biology

4.2.1. Calculation of IC_{50} value

HeLa cells were grown in DMEM supplemented with 10% FBS, 100 units/mL penicillin, and 100 μg/mL streptomycin in a humidified atmosphere containing 5% CO_2. Various concentrations of each compound were then added and incubated for 48 hours. Cell growth was determined using WST-8 cell counting kit (Dojindo) and IC_{50} value was calculated.

4.2.2. In vitro tubulin polymerization assay

MAPs free α,β-tubulin was purified from porcine brain using two cycles of polymerization-depolymerization in a high-molarity buffer as described previously.[16] 1 mg/mL α,β-tubulin, 1 M glutamate and 1 mM GTP were mixed in RB buffer (100 mM MES (pH 6.8), 1 mM EGTA, 0.5 mM $MgCl_2$). One of the compounds was then added and incubated for 10 min on ice. Samples were transferred into cuvette and tubulin polymerization was determined by monitoring the absorbance at 350 nm at 37 °C using a thermostatic spectrophotometer (Beckman Coulter). The IC_{50} values for O^6-benzyl glaziovianin A (**4**) and colchicine were calculated from final tubulin polymerization rate (control %) at 20 min of each concentration.

4.2.3. Competition assay

The competition assay of O^6-benzyl glaziovianin A (**4**) binding to tubulin with radiolabelled vinblastine or colchicine was monitored by the centrifugal gel filtration method. The reaction mixture (50 μL) containing 0.5 mg/mL (approx. 5 μM) tubulin, 50 nM [^3H]-labeled vinblastine or colchicine, 10% (v/v) DMSO and 100 μM mitotic inhibitor was incubated for 5 min at room temperature and processed by centrifugal gel filtration using Centri-Spin 20 (Princeton Separations).

4.2.4. K_d value calculation

Tryptophan fluorescence-based drug binding was performed as described in ref. 17 with minor modification. In briefly, 0.1 mg/mL α,β-tubulin and 1 mM GTP were mixed in RB buffer (100 mM MES (pH 6.8), 1 mM EGTA, 0.5 mM $MgCl_2$). Various concentrations of test compounds were then added and incubated for 30 min at room temperature. Samples were transferred into cuvette and tryptophan fluorescence of tubulin (excitation: 295 nm, emission: 310–450 nm) was monitored using RF-5300 (SHIMADZU). Dissociation constants were calculated from fitting curves of decreasing fluorescence using GraphPad Prizm.

4.2.5. Analysis of cell cycle progression

HeLa cells were grown in DMEM supplemented with 10% FBS, 100 units/mL penicillin and 100 μg/mL streptomycin in a humidified atmosphere containing 5% CO_2. Various concentrations of test compounds were then added and incubated for 18 hours. Cells were collected and fixed with 70% EtOH at –20 ℃. After wash with PBS, cells were stained with PI solution (0.2% NP-40, 0.1% trisodium citrate dehydrate, 71.1 μM propidium iodide and 10 μg/mL RNaseA) at 4 °C. DNA contents were analysed by cytometric analysis (PARTEC CyFlow PA; Partec GmbH, Munster, Germany). Cell populations of each cell cycle phase were calculated using Multi Cycle AV (PhoenixFlow Systems).

4.2.6. Observation of mitotic spindle

HeLa cells were grown in DMEM supplemented with 10% FBS, 100 units/mL penicillin and 100 μg/mL streptomycin in a humidified atmosphere containing 5% CO_2. Various concentrations of test compounds were then added and incubated for 6 hours. Cell growth was then fixed with cold MeOH (–20 °C). Cells were blocked with 0.5% bovine serum albumin and incubated with anti-α-tubulin antibody (1:500 dilution, Santa Cruz, sc-32293) for 1 h at 37 ℃. After staining with Alexa^{488}-conjugated anti-mouse IgG (1:2000 dilution, Invitrogen) for 30 min at 37 °C, coverslips were washed with PBS and mounted PBS containing 0.1 μg/mL DAPI. Microtubule cytoskeleton was observed under the LAS AF 6000 fluorescence microscope (Leica Microsystems).

Acknowledgments

This work was supported by Grants-in-Aid for Scientific Research on Innovative Areas ‘Chemical Biology of Natural Products’ (Grant Numbers JP23102014, JP23102013) and for Scientific Research (Grant Number JP16K07710) from the Ministry of Education, Culture, Sports, Science and Technology (MEXT)/Japanese Society for the Promotion of Science (JSPS). I.H. thanks the Okayama Foundation for Science and Technology, Kurata Grant awarded by the Kurata Memorial Hitachi Science and Technology Foundation, the NOVARTIS Foundation (Japan) for the Promotion of Science, the Naito Foundation, and the Suzuken Memorial Foundation for their financial support. We would also like to thank Prof. Elmar Schiebel (Zentrum für Molekulare Biologie der Universität Heidelberg) for his helpful discussion.

References and notes

1. Review: Kingston, D. G. I. *J. Nat. Prod*. **2009**, *72*, 507.
2. Uppuluri, S.; Knipling, L.; Sackett, D. L.; Wolff, J. *Proc. Natl. Acad. Sci. USA* **1993**, *90*, 11598.
3. Gigant, B.; Wang, C.; Ravelli, R. B. G.; Roussi, F.; Steinmetz, M. O.; Curmi, P. A.; Sobel, A.; Knossow, M. *Nature* **2005**, *435*, 519.
4. Rao, S.; He, L.; Chakravarty, S.; Ojima, I.; Orr, G. A.; Horwitz, S. B. *J. Biol. Chem.* **1999**, *274*, 37990.
5. Yokosuka, A.; Haraguchi, M.; Usui, T.; Kazami, S.; Osada, H.; Yamori, T.; Mimaki, Y. *Bioorg. Med. Chem. Lett*. **2007**, *17*, 3091.
6. Chinen, T.; Kazami, S.; Nagumo, Y.; Hayakawa, I.; Ikedo, A.; Takagi, M.; Yokosuka, A.; Imamoto, N.; Mimaki, Y.; Kigoshi, H.; Osada, H.; Usui, T. *ACS Chem. Biol.* **2013**, *8*, 884.
7. (a) Hayakawa, I.; Ikedo, A.; Kigoshi, H. *Chem. Lett.* **2007**, *36*, 1382; (b) Hayakawa, I.; Shioda, S.; Ikedo, A.; Kigoshi, H. *Bull. Chem. Soc. Jpn*. **2014**, *87*, 544.
8. (a) Ikedo, A.; Hayakawa, I.; Usui, T.; Kazami, S.; Osada, H.; Kigoshi, H. *Bioorg. Med. Chem. Lett*. **2010**, *20*, 5402; (b) Hayakawa, I.; Ikedo, A.; Chinen, T.; Usui, T.; Kigoshi, H. *Bioorg. Med. Chem*. **2012**, *20*, 5745; (c) There was a printing error in references 8a and 8b. The cytotoxicities of glaziovianin A and its derivatives were evaluated against HeLa cells (not HeLa S_3 cells).
9. In this paper, we name *O*-demethyl-*O*-alkyl glaziovianin derivatives as *O*-alkyl glaziovianins for simplification.
10. Tamura, S.; Yoshihira, K.; Tokumaru, M.; Zisheng, X.; Murakami, N. *Bioorg. Med. Chem. Lett*. **2010**, *20*, 3872.
11. (a) Monomethyl benzophenone **7** gave spectral data (^{1}H and ^{13}C NMR) in full agreement with the reported data[11b]; (b) O’Reilly, E.; Corbett, M.; Hussain, S.; Kelly, P. P.; Richardson, D.; Flitsch, S. L.; Turner, N. J. *Catal. Sci. Technol*. **2013**, *3*, 1490.
12. Hoshino, Y.; Miyaura, N.; Suzuki, A. *Bull. Chem. Soc. Jpn.* **1988**, *61*, 3008.
13. A plausible formation pathway of the O^6-benzyl glaziovianin A (**4**) is shown in the Supplementary data.
14. (a) We revealed that pure O^7-benzyl glaziovianin A (**3**) does not inhibit the polymerization of α,β-tubulin and shows the specific inhibition of γ-tubulin. O^7-Benzyl glaziovianin A (**3**) was named "gatastatin (gamma tubulin activity)"[14b]; (b) Chinen, T.; Liu, P.; Shioda, S.; Pagel, J.; Cerikan, B.; Lin, T.; Gruss, O.; Hayashi, Y.; Takeno, H.; Shima, T.; Okada, Y.; Hayakawa, I.; Hayashi, Y.; Kigoshi, H.; Usui, T.; Schiebel, E. *Nat. Commun*. **2015**, *6*, 8722.
15. From these results, previously synthesized O^7-modified glaziovianin A derivatives[8] had possibility of contaminating by-products. Hence, we have reevaluated cytotoxicity against HeLa cells of O^7-propargyl glaziovianin A, which was the most cytotoxic derivative in reference 8. The previous lot of O^7-propargyl glaziovianin A showed the same IC_{50} value as reported (IC_{50} = 0.17 μM). In contrast, cytotoxicity of a new lot of O^7-propargyl glaziovianin A (prepared by using modified synthetic route) is weaker (IC_{50} = 0.45 μM). Therefore, IC_{50} values of O^7-benzyl and propargyl glaziovianin A should be corrected as described in this paper, respectively.
16. Castoldi, M.; Popov, A. V. *Protein Expr. Purif.* **2003**, *32*, 83.
17. Sardar, P. S.; Maity, S. S.; Das, L.; Ghosh S. *Biochemistry* **2007**, *46*, 14544.

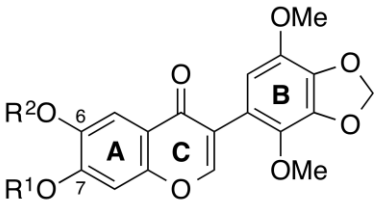

glaziovianin A (**1**) R^1 = Me, R^2 = Me

O^7-propargyl glaziovianin A (**2**) R^1 =  , R^2 = Me

O^7-benzyl glaziovianin A (gatastatin, **3**) R^1 = Bn, R^2 = Me

O^6-benzyl glaziovianin A (**4**) R^1 = Me, R^2 = Bn

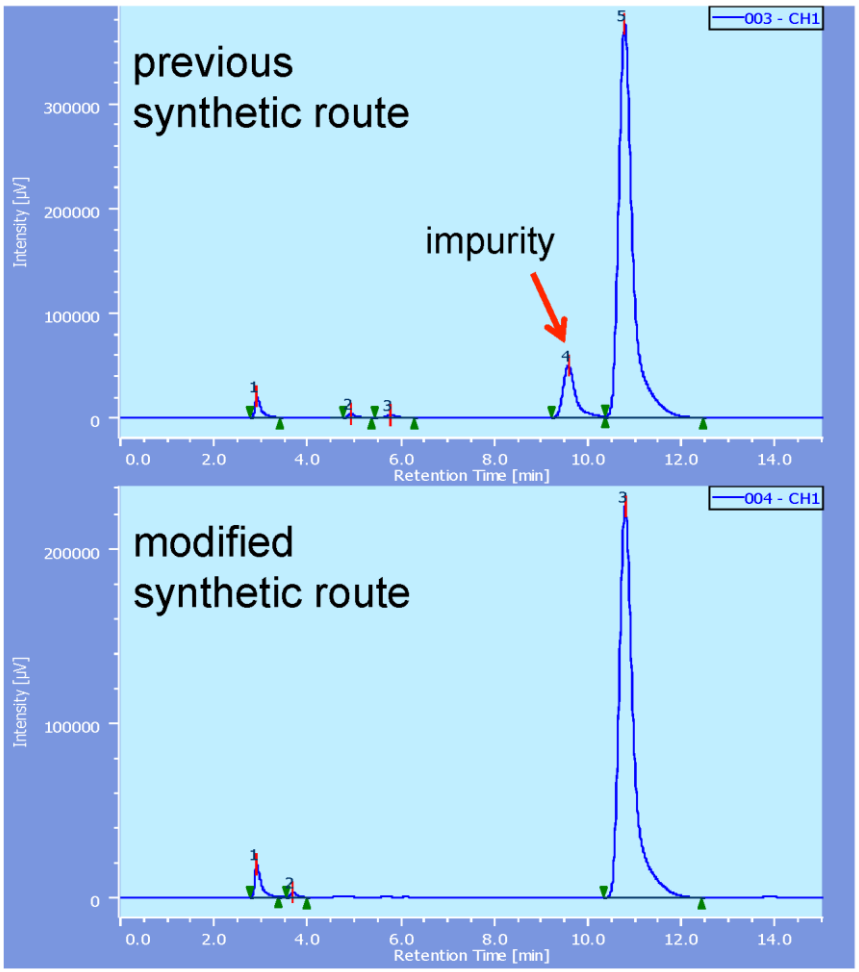

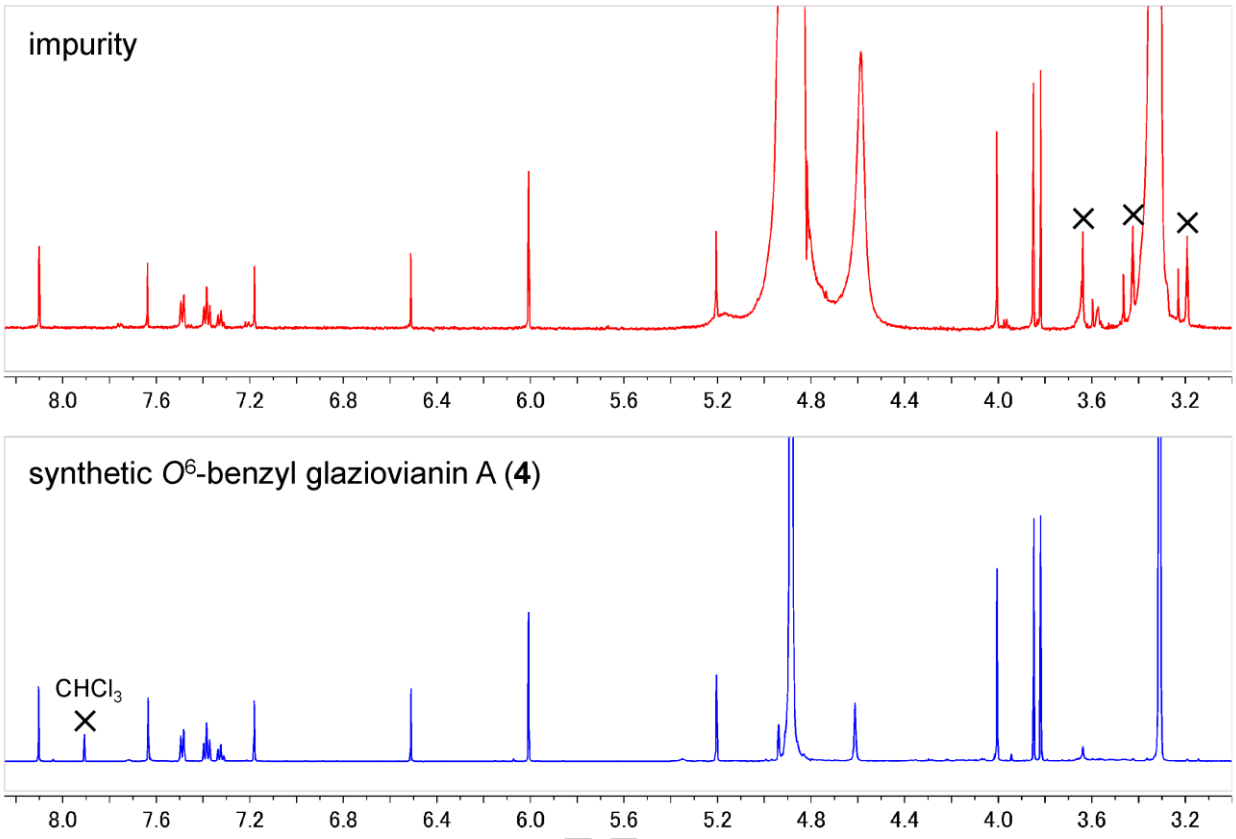

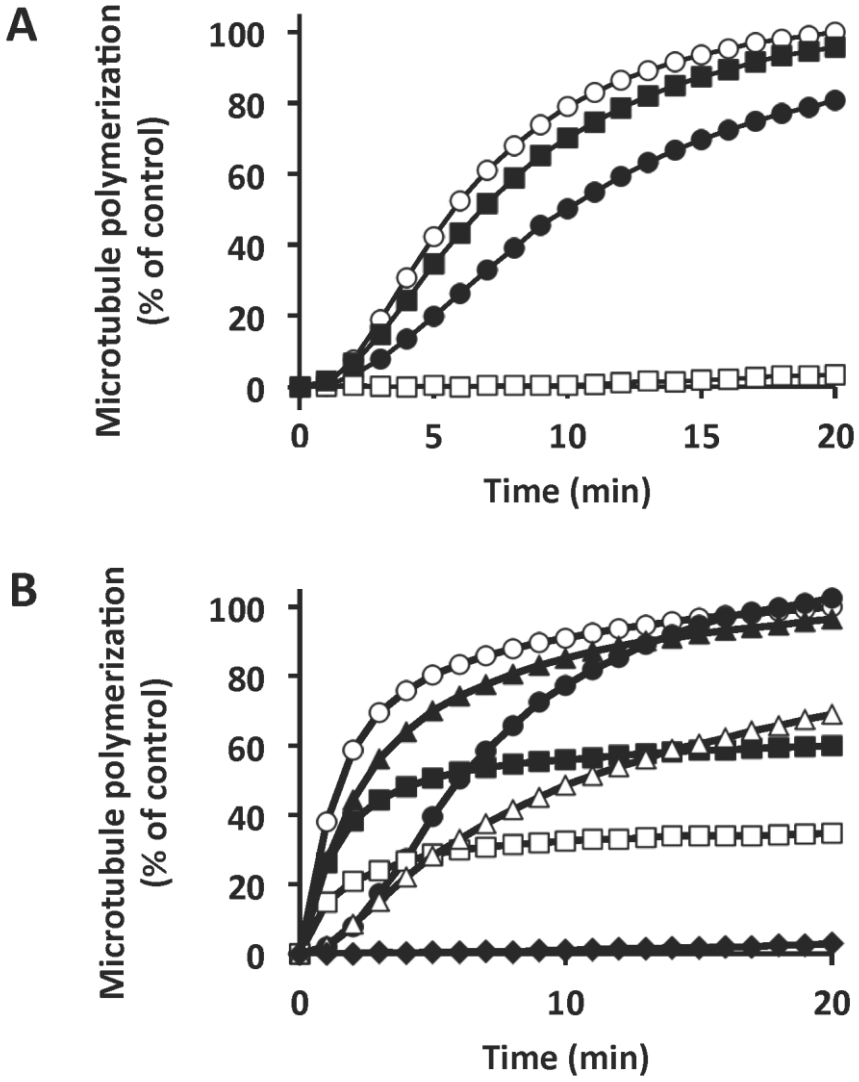

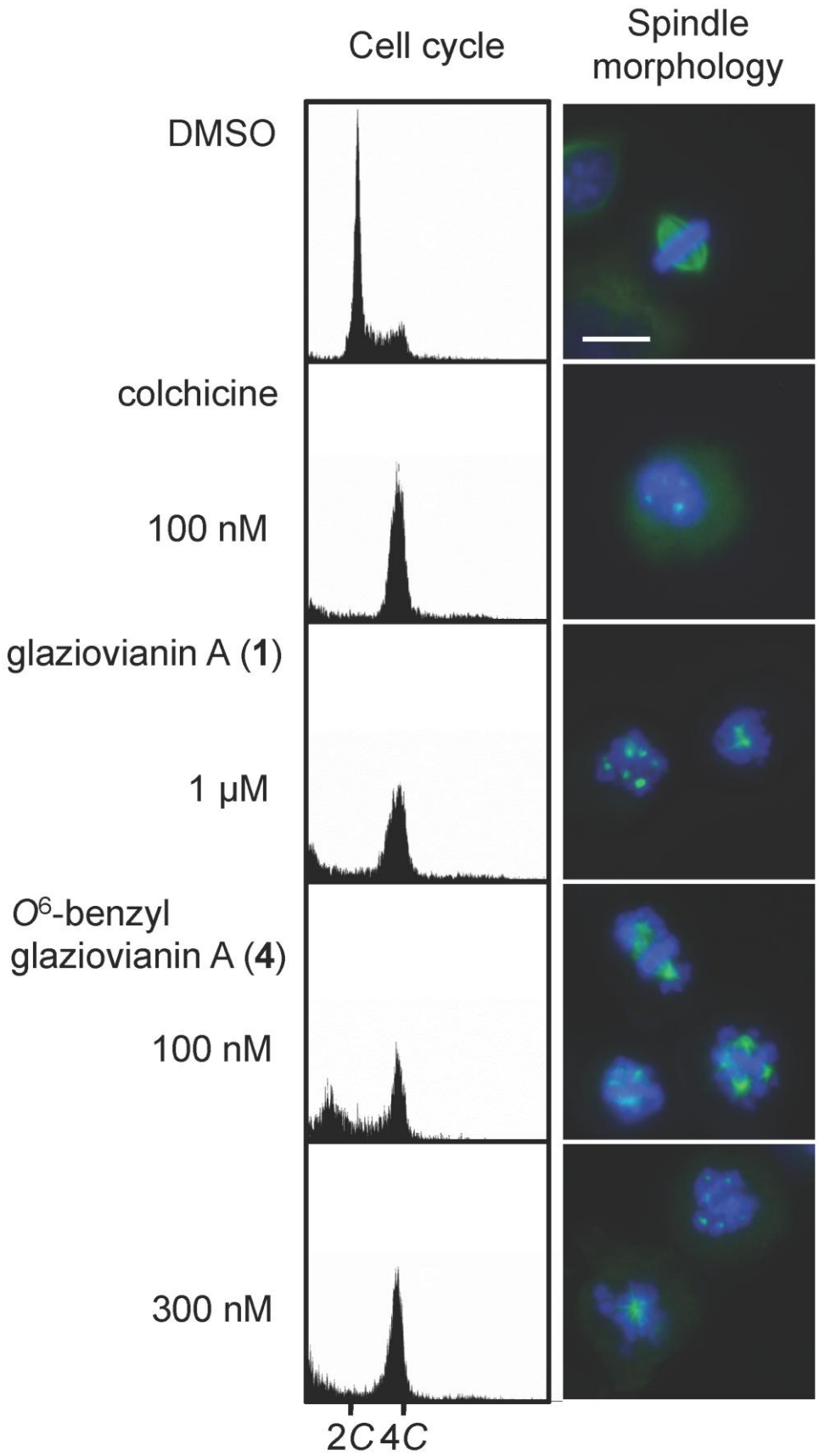

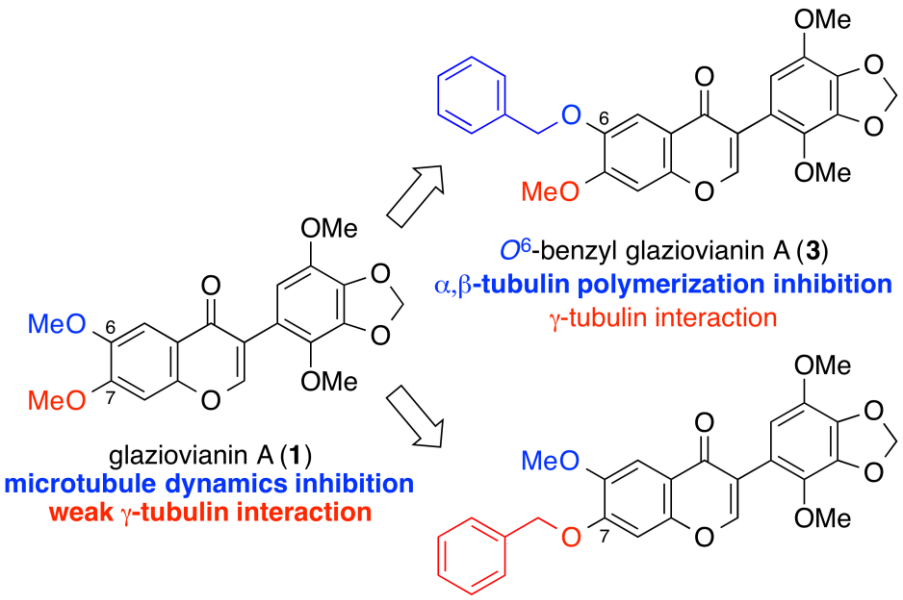

O^6-benzyl glaziovianin A (**3**)
α,β-tubulin polymerization inhibition
γ-tubulin interaction

glaziovianin A (**1**)
microtubule dynamics inhibition
weak γ-tubulin interaction

O^7-benzyl glaziovianin A (**4**)
γ-tubulin-specific interaction
and nucleation inhibition